Stars and their variability observed from space
C. Neiner, W. Weiss, D. Baade, E. Griffin, C. Lovekin, A. Moffat (eds)

DETERMINATION OF PRECISE STELLAR PARAMETERS OF KEPLER LEGACY TARGETS USING THE WHOSGLAD METHOD

M. Farnir[1], M.-A. Dupret[1], S.J.A.J. Salmon[1], A. Noels[1] and G. Buldgen[2]

Abstract. We developed a method, WhoSGlAd, that provides a comprehensive adjustment of solar like oscillations spectra. It allows for tighter constraints (up to four times smaller standard deviations than that of analogous ones). We take advantage of this new method and of the quality of the *Kepler* LEGACY data to highlight trends in the stellar parameters as well as the limitations of the current generation of stellar models.

Keywords: asteroseismology, stars: oscillations, stars: solar-type, stars: abundances, methods: numerical

1 Introduction

In the recent years, space missions such as *Kepler* (Borucki et al. 2010), CoRoT (Baglin et al. 2009) and BRITE (Weiss et al. 2014) provided a wealth of data of unprecedented quality. This has allowed asteroseismology to become a very efficient tool to constrain the stellar structure. Moreover, owing to the high quality of the data, it becomes possible to study acoustic glitches. Those are oscillating signatures in frequency spectra that are caused by a sharp variation* in the stellar structure. Therefore, they provide very localised and invaluable information. For example, several studies have taken advantage of the glitches to infer the surface helium content in solar-like pulsators, which cannot be measured by any other technique. The idea to use such glitches to constraint the stellar structure was first formulated by Gough (1990) and Vorontsov (1988). Since then, several studies including acoustic glitches have been carried out, among which we may cite Basu et al. (2004) and Verma et al. (2014). In a previous paper (Farnir et al. 2019), we have presented a new method, WhoSGlAd, to adjust simultaneously the signature of such glitches and the smoothly varying component of the oscillation spectrum. This method has the advantage of providing constraints correlated as little as possible thanks to the use of Gram-Schmidt's orthogonalisation process. Moreover, the standard deviation of the defined seismic indicators are up to four times smaller than the usual ones. In these proceedings, we shortly recall the principle of the WhoSGlAd method and present its application to the study of the *Kepler* LEGACY sample (Lund et al. 2017) as well to the in depth study of 16 Cygni A.

2 Principle

2.1 Mathematical description

This section consists of a very brief description of the WhoSGlAd method's principle. More information may be found in Farnir et al. (2019). To describe a set of observed frequencies, ν_{obs}†, we built a euclidean vector space of functions. The following scalar product is defined:

$$\langle \boldsymbol{x} | \boldsymbol{y} \rangle = \sum_{i=1}^{N} \frac{x_i y_i}{\sigma_i^2}, \tag{2.1}$$

[1] Institut d'Astrophysique et Géophysique de l'Université de Liège, Allée du 6 août 17, 4000 Liège, Belgium
[2] Observatoire de Genève, Université de Genève, 51 Ch. Des Maillettes, 1290 Sauverny, Switzerland
*compared to the wavelength of the incoming wave
†We here denote by the *obs* subscript, frequencies to be adjusted, be them observed or model frequencies.

where $\boldsymbol{x}$ and $\boldsymbol{y}$ are two sets of N frequencies and σ_i are the individual standard deviations. In this vector space we represent the smooth part of the oscillation spectrum as polynomials in the radial order n and the glitch part as oscillating functions linearised for the fitted coefficients. Then, using the Gram-Schmidt's orthogonalisation process, we build an orthonormal basis over this vector space. If we write $p_j(n,l)$ the former basis elements, $q_{j_0}(n,l)$ the orthonormal basis elements and $R^{-1}_{j,j0}$ the transformation matrix, we have:

$$q_{j_0}(n,l) = \sum_{j \leq j_0} R^{-1}_{j,j_0} p_j(n,l). \tag{2.2}$$

Finally, using the scalar product 2.1, we project the frequencies over the successive basis elements. The fitted frequencies are thus:

$$\nu_f(n,l) = \sum_j a_j q_j(n,l), \tag{2.3}$$

where a_j are the fitted coefficients and $q_j(n,l)$ the orthonormal basis elements. It is essential to note that, owing to the orthonormalisation, all the coefficients a_j are completely independent of each other. Therefore, while the glitch and smooth components are treated simultaneously they are fully uncorrelated.

2.2 Useful seismic indicators

Combining in a clever way the adjusted coefficients, we may construct seismic indicators as uncorrelated as possible for the stellar structure that are proxies of the 'usual' ones.

Large separation: At first order, the smooth part of the spectrum is approximated by a straight line. For a given spherical degree, the slope of this line is the large separation for this degree. In our formulation, we obtain[‡]

$$\Delta_l = a_{l,1} R^{-1}_{l,1,1} \tag{2.4}$$

Averaging this quantity over the range of observed spherical degrees, we get:

$$\Delta = \frac{\sum_l a_{l,1}/R^{-1}_{l,1,1}}{\sum_l 1/\left(R^{-1}_{l,1,1}\right)^2} \tag{2.5}$$

Small separation ratios: Analogous to Roxburgh & Vorontsov (2003), we may define averaged small separation ratios as:

$$\hat{r}_{0,l} = \frac{\bar{\nu_0} - \bar{\nu_l}}{\Delta_0} + \bar{n_l} - \bar{n_0} + \frac{l}{2}, \tag{2.6}$$

where the overlined symbols represent the mean value of those quantities calculated using our scalar product. We show in Farnir et al. (2019) that these ratios are almost independent of the surface effects, as expected from Roxburgh & Vorontsov (2003).

Large separation ratios: We define:

$$\Delta_{0l} = \frac{\Delta_l}{\Delta_0} - 1 \tag{2.7}$$

It is straightforward to show that it represents the mean slope of r_{010}, which is the combination of the small separation ratios r_{01} and r_{10} (Roxburgh & Vorontsov 2003).

Helium glitch amplitude: We define the amplitude of the helium glitch, $\delta\nu_{\mathrm{He}}$, as the norm of the helium glitch term, i.e.:

$$A_{\mathrm{He}} = \|\delta\nu_{\mathrm{He}}\| = \sqrt{\sum_j a^2_{j,\mathrm{He}}}. \tag{2.8}$$

[‡]Note that, for the smooth part, the j index has been separated into the spherical degree l and the polynomial degree k, as we have different polynomials for each spherical degree.

3 Applications

3.1 Models

Unless specified otherwise, every model was constructed using the CLES stellar evolution code (Scuflaire et al. 2008b) with the AGSS09 solar chemical mixture (Asplund et al. 2009), the OPAL opacity table (Iglesias & Rogers 1996) combined with that of Ferguson et al. (2005) at low temperatures, the FreeEOS software to generate the equation of state table (Cassisi et al. 2003) and the reactions rates prescribed by Adelberger et al. (2011). We also used the mixing length theory (Cox & Giuli 1968), with the solar calibrated value of $\alpha_{\rm MLT} = l/H_p = 1.82$ (where l is the mixing length and H_p the pressure scale height), to parametrise the mixing inside convective regions. The microscopic diffusion of elements was included and treated as in Thoul et al. (1994). Moreover, the temperature conditions above the photosphere were determined using an Eddington $T(\tau)$ relationship, τ being the optical depth. Finally, the model frequencies were calculated using the LOSC oscillation code (Scuflaire et al. 2008a) which were corrected for the surface effects according to Kjeldsen et al. (2008)'s prescription using the a and b coefficients fitted by Sonoi et al. (2015).

3.2 The Kepler LEGACY sample

The *Kepler* LEGACY sample consists of 66 main sequence solar-like stars which have been observed by the *Kepler* telescope for at least one continuous year (Lund et al. 2017). This is therefore the best data available to the asteroseismology of main sequence solar-like pulsators.

For each star in the sample, we tried to provide a fitted model to the observed seismic indicators defined in the previous section and built over the frequencies from Lund et al. (2017). To do so, we first used the AIMS algorithm (Rendle et al. 2019) to provide initial guesses that were then used as starting points by a Levenberg-Marquardt algorithm.

The constraints used are the following seismic indicators: Δ, $\hat{r}_{01}$, $\hat{r}_{02}$, Δ_{01} and $A_{\rm He}$ and the metallicity. The free parameters are: the mass, age, initial hydrogen and metal abundances and the overshooting parameter.

From the whole sample, only 18 stars were properly fitted, with a $\chi^2 = \sum_i \left(\frac{y_{{\rm th},i} - y_{{\rm obs},i}}{\sigma_{{\rm obs},i}} \right)^2 \leq 40$. The results are shown in Figs. 1 and 2. Figure 1 shows the initial helium content as a function of the initial metallicity. We observe a correlation which could be a clue of a galactic enrichment. In Fig.2 we show the adjusted overshooting parameter versus the stellar mass. We do not observe a correlation between those two quantities as expected from Claret & Torres (2019). However, the range of masses depicted in their Fig. 10 is much broader than ours and the apparent absence of correlation could result from our restricted mass range. Therefore, to validate both observations, it will be necessary to provide a proper adjustment for as many stars from the sample as possible.

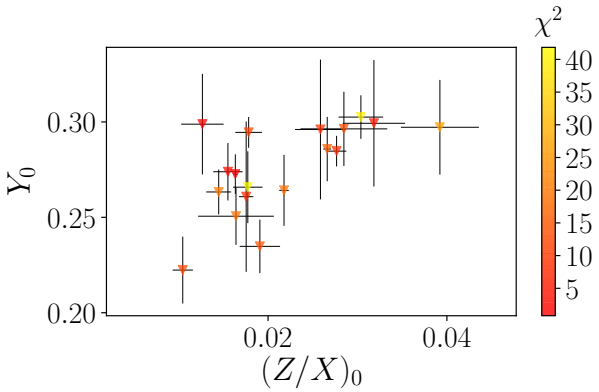

Fig. 1: Best fit values for the initial helium abundance as a function of the initial metallicity. The color code represents the χ^2 value for each model.

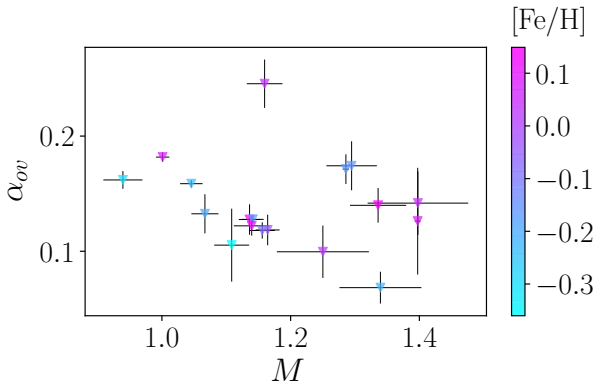

Fig. 2: Best fit values for the step overshooting parameter as a function of the mass. The color code represents the metallicity of the models.

3.3 Application to 16 Cygni A

In the previous subsection, we showed adjustments that were done by considering only one set of physical ingredients. To properly understand the dependency of the stellar parameters on the physics as well as to provide proper standard deviations for these parameters, one has to test different physical ingredients. This is what we did for the specific case of 16 Cyg A. We show in Fig. 3 the results for the different choices of microphysics we considered. The frequencies from which we built our seismic indicators were those determined by Davies et al. (2015). We calculated the models shown in the figure by changing one microphysical ingredient from the reference described in Sec. 3.1 at a time. The reference is shown in black. The considered variations were: the GN93 solar reference (Grevesse & Noels 1993) (in red), the opacity table from the opacity project OP (Badnell et al. 2005) (in green), the LANL/OPLIB opacity table (Colgan et al. 2016) (in blue), the CEFF equation of state (Christensen-Dalsgaard & Daeppen 1992) (in yellow), the OPAL05 equation of state (Rogers & Nayfonov 2002) (in magenta), the inclusion of turbulent mixing (in cyan) following the relation $DDT = D_{\rm turb}\left(\frac{\rho}{\rho_0}\right)^n + D_{ct}$, where ρ is the density, ρ_0 the surface density and $D_{\rm turb}$, n and D_{ct} were fixed at -7500, -3 and 0 respectively (Proffitt & Michaud 1991). A reduced value of 1.7 for the mixing length parameter (in light green) was also considered. We used Δ, $\hat{r}_{01}$, $\hat{r}_{02}$ and $A_{\rm He}$ as constraints and the mass, age, initial helium abundance and metallicity as free parameters.

We observe that, given the current precision of both the data and the method, it becomes possible to discriminate between different choices of input physics. We also show with a grey box the luminosity (deduced from the interferometric radius) and effective temperature (White et al. 2013). These constraints were not included during the fit, we merely show the discrepancy of the results with those. Only a few models lie in the box, one of them relying on non classical physics (the cyan model includes turbulent mixing). This clearly illustrates the limitations of the forward approach for the stellar modelling as well as that of our knowledge about the stellar structure. To further improve our results and highlight the necessary improvements to the stellar models, one should consider making use of inverse techniques as in Buldgen et al. (2016).

4 Conclusions

The WhoSGlAd method allows us to provide a comprehensive adjustment of solar-like pulsators oscillations spectra as a whole (glitch and smooth parts) and to put tighter seismic constraints (up to four time smaller than 'classical' ones) on the stellar structure. Combined with the precision of the *Kepler* LEGACY data, it becomes possible to observe trends over the whole sample (we note a correlation between the initial helium content and the initial metallicity) as well as the limitations of the current stellar models. It therefore becomes necessary to refine those by, for example, improving the treatment of convection or including non-standard physics (e.g. turbulent mixing, revised abundances and opacities). Moreover, to go even further in the modelling, combining the promising WhoSGlAd method with inverse techniques may be of great help. Finally, the adaptation of the method to the more complex case of subgiants exhibiting mixed modes will be a natural step as those present the regularities of p and g modes, which are well suited for such an approach.

M.F. is supported by the FRIA (Fond pour la Recherche en Industrie et Agriculture) - FNRS PhD grant. S.J.A.J.S. is funded by ARC grant for Concerted Research Actions, financed by the Wallonia-Brussels Federation. G. Buldgen is supported by the Swiss National Science Foundation (project number 200020 172505)

References

Adelberger, E. G., García, A., Robertson, R. G. H., et al. 2011, Reviews of Modern Physics, 83, 195

Asplund, M., Grevesse, N., Sauval, A. J., & Scott, P. 2009, ARA&A, 47, 481

Badnell, N. R., Bautista, M. A., Butler, K., et al. 2005, MNRAS, 360, 458

Baglin, A., Auvergne, M., Barge, P., et al. 2009, in IAU Symposium, Vol. 253, Transiting Planets, ed. F. Pont, D. Sasselov, & M. J. Holman, 71–81

Basu, S., Mazumdar, A., Antia, H. M., & Demarque, P. 2004, MNRAS, 350, 277

Borucki, W. J., Koch, D., Basri, G., et al. 2010, in Bulletin of the American Astronomical Society, Vol. 42, American Astronomical Society Meeting Abstracts #215, 215

Buldgen, G., Reese, D. R., & Dupret, M. A. 2016, A&A, 585, A109

Cassisi, S., Salaris, M., & Irwin, A. W. 2003, ApJ, 588, 862

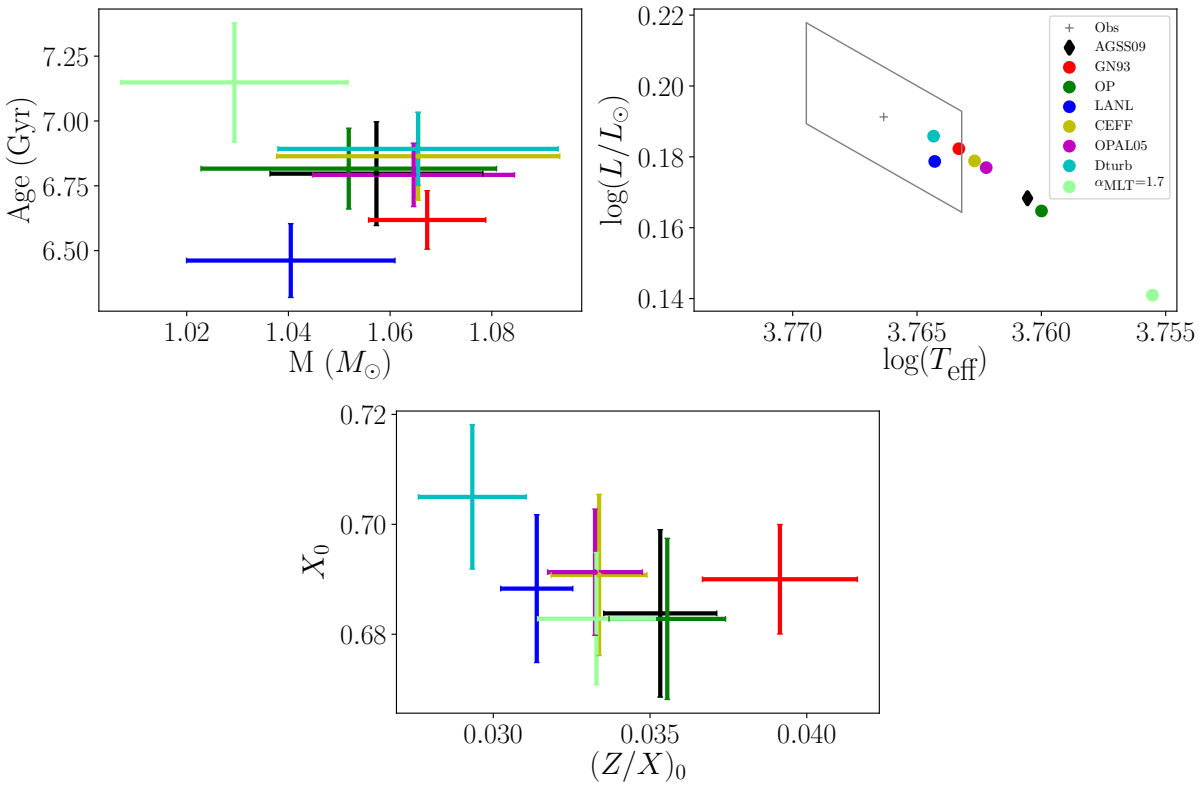

Fig. 3: Ensemble of 16Cyg A best fit models represented in an age - mass diagram (upper left panel), HR diagram (upper right panel) and inial hydrogen - metallicity diagram (lower panel). The different choices of microphysics are represented by the colors. The luminosity (deduced from the interferometric radius) and effective temperature (White et al. 2013) observed values and standard deviations are represented by the grey box in the upper right panel.

Christensen-Dalsgaard, J. & Daeppen, W. 1992, A&A Rev., 4, 267
Claret, A. & Torres, G. 2019, ApJ, 876, 134
Colgan, J., Kilcrease, D. P., Magee, N. H., et al. 2016, ApJ, 817, 116
Cox, J. P. & Giuli, R. T. 1968, Principles of stellar structure
Davies, G. R., Chaplin, W. J., Farr, W. M., et al. 2015, MNRAS, 446, 2959
Farnir, M., Dupret, M. A., Salmon, S. J. A. J., Noels, A., & Buldgen, G. 2019, A&A, 622, A98
Ferguson, J. W., Alexander, D. R., Allard, F., et al. 2005, ApJ, 623, 585
Gough, D. O. 1990, in Lecture Notes in Physics, Berlin Springer Verlag, Vol. 367, Progress of Seismology of the Sun and Stars, ed. Y. Osaki & H. Shibahashi, 283
Grevesse, N. & Noels, A. 1993, in Origin and Evolution of the Elements, ed. N. Prantzos, E. Vangioni-Flam, & M. Casse, 15–25
Iglesias, C. A. & Rogers, F. J. 1996, ApJ, 464, 943
Kjeldsen, H., Bedding, T. R., & Christensen-Dalsgaard, J. 2008, ApJ, 683, L175
Lund, M. N., Silva Aguirre, V., Davies, G. R., et al. 2017, ApJ, 835, 172
Proffitt, C. R. & Michaud, G. 1991, ApJ, 380, 238
Rendle, B. M., Buldgen, G., Miglio, A., et al. 2019, MNRAS, 484, 771
Rogers, F. J. & Nayfonov, A. 2002, ApJ, 576, 1064
Roxburgh, I. W. & Vorontsov, S. V. 2003, A&A, 411, 215
Scuflaire, R., Montalbán, J., Théado, S., et al. 2008a, Ap&SS, 316, 149
Scuflaire, R., Théado, S., Montalbán, J., et al. 2008b, Ap&SS, 316, 83
Sonoi, T., Samadi, R., Belkacem, K., et al. 2015, A&A, 583, A112
Thoul, A. A., Bahcall, J. N., & Loeb, A. 1994, ApJ, 421, 828

Verma, K., Faria, J. P., Antia, H. M., et al. 2014, ApJ, 790, 138

Vorontsov, S. V. 1988, in IAU Symposium, Vol. 123, Advances in Helio- and Asteroseismology, ed. J. Christensen-Dalsgaard & S. Frandsen, 151

Weiss, W. W., Rucinski, S. M., Moffat, A. F. J., et al. 2014, PASP, 126, 573

White, T. R., Huber, D., Maestro, V., et al. 2013, MNRAS, 433, 1262